The International Journal of Advanced Manufacturing Technology (2018) 99:1225–1234
https://doi.org/10.1007/s00170-018-2539-z

ORIGINAL ARTICLE

Creep behavior analysis of additively manufactured fiber-reinforced components

M. Mohammadizadeh[1] · I. Fidan[2] · M. Allen[3] · A. Imeri[1]

Received: 7 June 2018 / Accepted: 7 August 2018 / Published online: 18 August 2018

Abstract

This research study reports the creep behavior analysis of the new composite materials manufactured by 3D printing technology. Nylon was used as a polymer matrix, and carbon fiber, Kevlar, and fiberglass were used as reinforcing agents. Since the properties of 3D-printed components are usually insufficient for robust engineering applications, adding reinforcing fibers improves the performance of these components for several engineering applications. Fiber-reinforced additive manufacturing (FRAM) is an almost 4-year-old technology. Additionally, there is not sufficient research on the behavior of FRAM components specifically at high temperatures. Therefore, the investigation of the high-temperature behavioral analysis of FRAM components was focused on in this study. Creep properties of the composite specimens reinforced by different fibers were measured by the dynamic mechanical thermal analysis system. The statistical analyses were conducted to analyze the experimental data using mathematical models. The microstructural analysis was performed to further investigate parts' morphology, 3D printing quality, and fracture mechanisms. The results indicated that the creep compliance of reinforced composite specimens was significantly improved in comparison with pure nylon. Overall, this paper presents quantitative creep analysis results demonstrating the capabilities of FRAM components to be used for several engineering applications.

Keywords Fiber-reinforced additive manufacturing · Creep · Microstructural analysis · Statistical analysis

1 Introduction

3D printing is an emerging technology used to build three-dimensional structures based on a layer-by-layer deposition. The revolution of this technology is remarkable, and it is evolving toward producing materials such as polymer composites for practical use [1, 2]. 3D printing technology has advantages including a short production time, little material waste, low price, and an extended ability to print a complex shape [1–3]. Among various 3D printing methods, fused deposition modeling (FDM) is a simple, low-cost, and fairly reliable technology that uses a filament of polymer threaded through a heated extruder nozzle and deposits fused material on a platform in layers to form a shape. FDM has been extensively researched to improve the product performance and functionality for various applications such as automobile [4], medical implants [5], telecommunications [6], and more [7–9]. Fiber-reinforced polymer composites consist two or more different materials and thus possess a broad range of mechanical properties that can be engineered for different applications [10]. Lightweight, low price, and good thermomechanical properties make fiber-reinforced 3D-printed polymer composites great candidates to replace metals in engineering applications especially automotive and aerospace fields [1, 8]. In addition to having high strength and possibility for high production rates, thermoplastic FRAMs are reusable,

✉ I. Fidan
ifidan@tntech.edu

M. Mohammadizadeh
mmohammad42@students.tntech.edu

M. Allen
mallen@tntech.edu

A. Imeri
aimeri42@students.tntech.edu

[1] Mechanical Engineering Department and Center for Manufacturing Research, Tennessee Technological University, Cookeville, TN, USA

[2] Manufacturing and Engineering Technology Department, Tennessee Technological University, Cookeville, TN, USA

[3] Mathematics Department, Tennessee Technological University, Cookeville, TN, USA

environmentally friendly, and widely used materials, finding applications especially in automotive industry [2]. Moreover, such materials are viscoelastic, particularly at elevated temperatures such as in automobiles where under the hood, temperature can increase up to 130 °C because of the engine temperature and weather conditions [2].

FRAM technology itself is almost 4 years old [11]. The niche of this study is on continuous fiber-reinforced 3D-printed composites. The literature review performed by the authors indicates that there is no quality research performed to measure the creep behaviors of the additively manufactured fiber-reinforced components although there are several studies on fiber-reinforced concrete [12], soil [13], and polymer [14]. This pioneering research fills such a gap and contributes the body of knowledge of creep properties of such continuous fiber-reinforced 3D-printed composites. Different materials are added to polymers in order to improve thermal, mechanical, electrical, and other properties. In particular, reinforcing fibers, such as carbon fiber (CF), are considered to enhance mechanical properties and thermal stability of polymer. Nylon, as one of the most practical thermoplastic polymers in different industries, can be reinforced by filaments to improve mechanical and thermal properties. The satisfactory mechanical properties of nylon make it a promising candidate for 3D printing, while reinforcing fibers improve properties. Understanding the effect of temperature on mechanical properties of composite parts is of great importance due to the strong dependence of mechanical properties on temperature and a large number of applications at elevated temperatures.

Recently, some researchers have studied mechanical properties of 3D-printed polymer composites [8, 15–19]. Mechanical properties generally decrease almost linearly with increasing temperature. Common failure mechanisms of polymer composites at elevated temperatures under the above loading conditions includes crazing, matrix yielding, interfacial debonding, and fiber pullout [20]. Because the field of FRAM is a new production technology, there is a limited research about the mechanical behavior of additively manufactured fiber-reinforced components. The objective of this research is to study the creep behavior of these materials at room and high temperature. Creep is a continuing deformation of the material under constant stress over an extended period of time. Polymers and consequently polymer composites have both long-term and short-term properties. Most of the applications of reinforced polymer composites are at temperatures higher than their glass transition temperature (Tg). Therefore, studying creep behavior of 3D-printed polymer composites at high temperatures is of great importance. Polymers are sensitive to temperature and strain rate. So, most of the mechanical tests of polymers is evaluating viscoelastic behavior under applied load at desired temperature [21]. Creep behavior of 3D-printed polymer composites has been studied extensively by researchers. Zhang et al. [22] studied tensile, creep, and fatigue behaviors of 3D-printed acrylonitrile butadiene styrene (ABS). Imeri et al. studied fatigue behavior of fiber-reinforced 3D-printed polymer composites [23]. Niaza et al. [9] studied creep and impact properties of 3D-printed polylactic acid (PLA) used as scaffolds. An increase in temperature has been observed to decrease creep resistance and accelerate creep fracture process, which is because of increased macromolecular mobility of polymer chains with increasing temperature. Fiber reinforcement reduces both the creep strain and the creep rate; however, insufficiently bound fibers lose their reinforcing role and turn into potential defects, thus, accelerating creep. The prevailing creep damage mechanism is crazing perpendicular to the stress direction, which typically starts at the fiber-matrix interface [2]. Creep behavior of conventional polymer composites has been studied extensively [24]. To the best of our knowledge, this is the first research study that focuses on thermomechanical properties of FRAM and extended with microstructure analysis. Studying creep behavior is more significant in materials that are subjected to heat for long periods.

Inclusion of reinforcing fibers into polymer matrix is considered as a solution to improve mechanical properties of 3D-printed polymer while benefiting from advantages of 3D printing technology such as flexibility in design and low cost [25]. In this work, creep behavior of FRAM at different temperatures is investigated. Specimens of nylon were reinforced using three different fibers containing CF, fiberglass (FG), and Kevlar. A temperature range has been designed to cover temperatures needed for application in automotive industry. Statistical analysis determined the difference in the creep models for the composites containing different fibers. To further investigate the structure of produced parts, microscopic imaging of specimens was analyzed.

2 Methodology

Nylon, CF, FG, and Kevlar were purchased from Markforged Company. Nylon was used as polymer matrix, and fibers were used for reinforcement. The 3D printer used is a Markforged Mark Two (MKF) printer in conjunction with Eiger slicer software. The printer has dual head extrusion, one for polymer matrix and one for reinforcing fibers. 3D-printed composites are new field of study and studying the effect of printing condition on properties is under research [24, 26]. Printing parameters have significant effect on 3D-printed polymers and need to be set precisely. The printing parameters are as follows: extrusion head temperature was set in the range of 265–270 °C; the layer thickness was 0.1 mm for nylon, FG,

and Kevlar filament and 0.125 mm for CF; and internal contour with 50% density. Creep test was done using TA Instrument DMA tester model Q800 according to the ASTM standard D2990-17 for the creep test of polymer composite specimens [27]. All specimens were allowed to equilibrate at least for 3 min in test temperature. The constant stress of 2.7 MPa was applied on the samples parallel to fiber axis. Loading was continued for 60 min according to ASTM D-2990-17, and strain was monitored as a function of time. Then, the stress was released to allow the specimen to recover for duration of 60 min, and strain was recorded again. For precision purposes, each test was conducted twice. The creep specimens used in this study are designed based on the specifications outlined by creep machine manufacturer. Samples were rectangles with dimensions of 10 by 8 mm, with a 0.5-mm thickness. The specimens were designed using SolidWorks 2016 software and were printed with the MKF. Due to moisture sensitivity, the nylon filament was kept in a water-tight Pelican 1430 dry box. The filaments were forwarded in the extrusion heads using stepper motors. The extrusion head temperature and bed temperature were set between 265 and 270 °C and 39–40 °C, respectively. At this temperature, while passing through the extrusion head, the base material turned into a molten state and starts to solidify as soon as it leaves the nozzle. The fiber reinforcement materials do not melt at that temperature but were laid down horizontally, layer by layer in the nylon matrix. The first and last layer of the part is made up of nylon. The printing process continued layer by layer until the specimen was completed. For the nylon material, the filament came in a form of 1.75 mm diameter, but the layer height that the printer could print was 0.125 mm. Kevlar and FG came in diameters of 0.3 mm, while the CF came in a diameter of 0.35 mm. Nylon was printed with rectilinear infill, in which the first layer angle was 45° with respect to the axial direction. Then, the next four layers of fiber filament were printed with 0° and the last layer was nylon filament with 45° in opposite angle compared with the first layer. Schematic view of nylon and fiber arrangement is shown in Fig. 1. Samples were dried for 2 h in vacuum after printing and stored in an airtight package to minimize moisture absorption. The top view of the printed samples is shown in Fig. 2.

3 Results and discussion

3.1 Creep analysis

Creep compliance and creep recovery were measured using three-point bending DMA machine. Static force was applied on sample and held constant for 60 min at test temperature. The dimension change was monitored during the 60 minutes to determine creep compliance. Then, the applied load was turned off, and the dimension change was measured again to measure creep recovery during the next 60 min. Strain of composite samples during the time in two different temperatures is shown in Fig. 3. As can be seen, the composite shows viscoelastic behavior to the creep test. At first, the sample demonstrates a large strain, and then the strain rate gradually decreases as time passes. As the application of force stops, the part begins to recover. Initially, strain recovery rate is high and gradually decreases to lower strain rates as time passes, as shown in each graph of Fig. 3 for the second 60 min.

Figure 3a–d shows that increasing temperature from room temperature to 100 °C increases the strain for each specimen. Inclusion of reinforcing fibers to the nylon improves mechanical properties to withstand against creep deformation. Pure nylon shows more than 2.5% strain at 100 °C, which is almost 25 times bigger than the strain of polymers reinforced with fibers at same temperature, as shown in Fig. 3a–d. At 100 °C, nylon-FG shows strain 0.12% (Fig. 3c) while nylon-CF (Fig. 3b) and nylon-Kevlar (Fig. 3d) show 0.095 and 0.105% strain, respectively. For composite samples, as temperature increases from room temperature to 100 °C, strain rate becomes twice while for pure nylon, this increase is 20%.

Creep compliance and creep recovery results of FRAM specimens at room temperature and 100 °C are shown in Fig. 4. As can be seen in Fig. 4a–d, inclusion of reinforcing

Fig. 1 Schematic view of matrix and fiber arrangement in 3D-printed parts

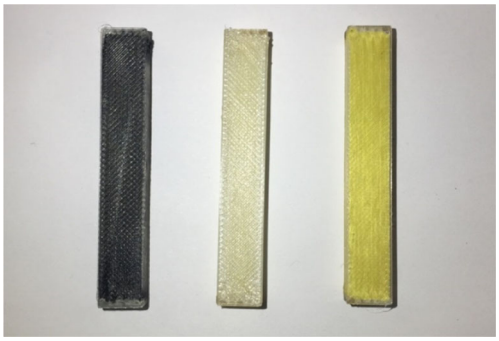

Fig. 2 Top view of the printed polymer composite specimens (from left to right: nylon-CF, nylon-FG, nylon-Kevlar)

fibers improves creep resistance almost 40 times compared with that of pure nylon specimens. So, the reinforcing fiber plays an important role to improve mechanical properties in FRAM specimens. Comparing test results at room temperature and 100 °C shows that with increasing temperature, creep also increases due to weakening of bonding strength and consequently decrease in stress transfer at the interface.

As shown in the magnification part of figures, at room temperature and 100 °C, nylon-FG showed creep amount higher than nylon-Kevlar and after them, nylon-CF showed lowest creep amount. There are two factors controlling the creep behavior of composite. Fiber-polymer interaction is the most important factor governing the creep properties. Good interaction of polymer-fiber causes low creep of specimens. Although creep results for FRAM specimens are close to each other, as magnification part of figure shows, it seems that interaction of nylon-CF is strongest and therefore has the lowest creep deformation. Following, it seems that nylon-Kevlar and nylon-FG have lower interaction strength respectively. Based on the mixture law, fiber and matrix's mechanical properties determine composites' mechanical behavior according to the weight percent of each component. This may be the reason why nylon-CF shows lower creep amount,

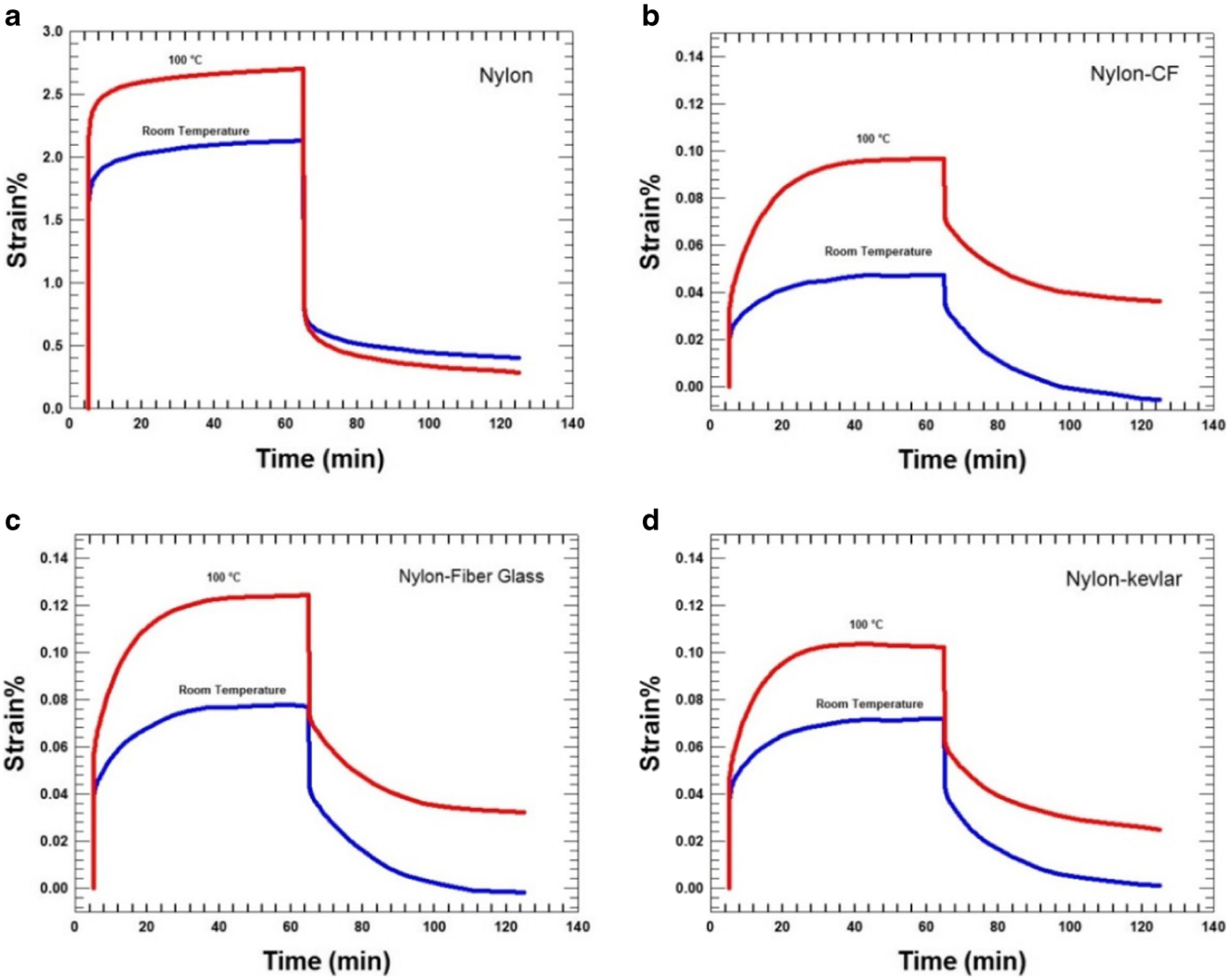

Fig. 3 Strain of 3D-printed polymer composites at two different temperatures. **a** Nylon. **b** Nylon-CF. **c** Nylon-FG. **d** Nylon-Kevlar

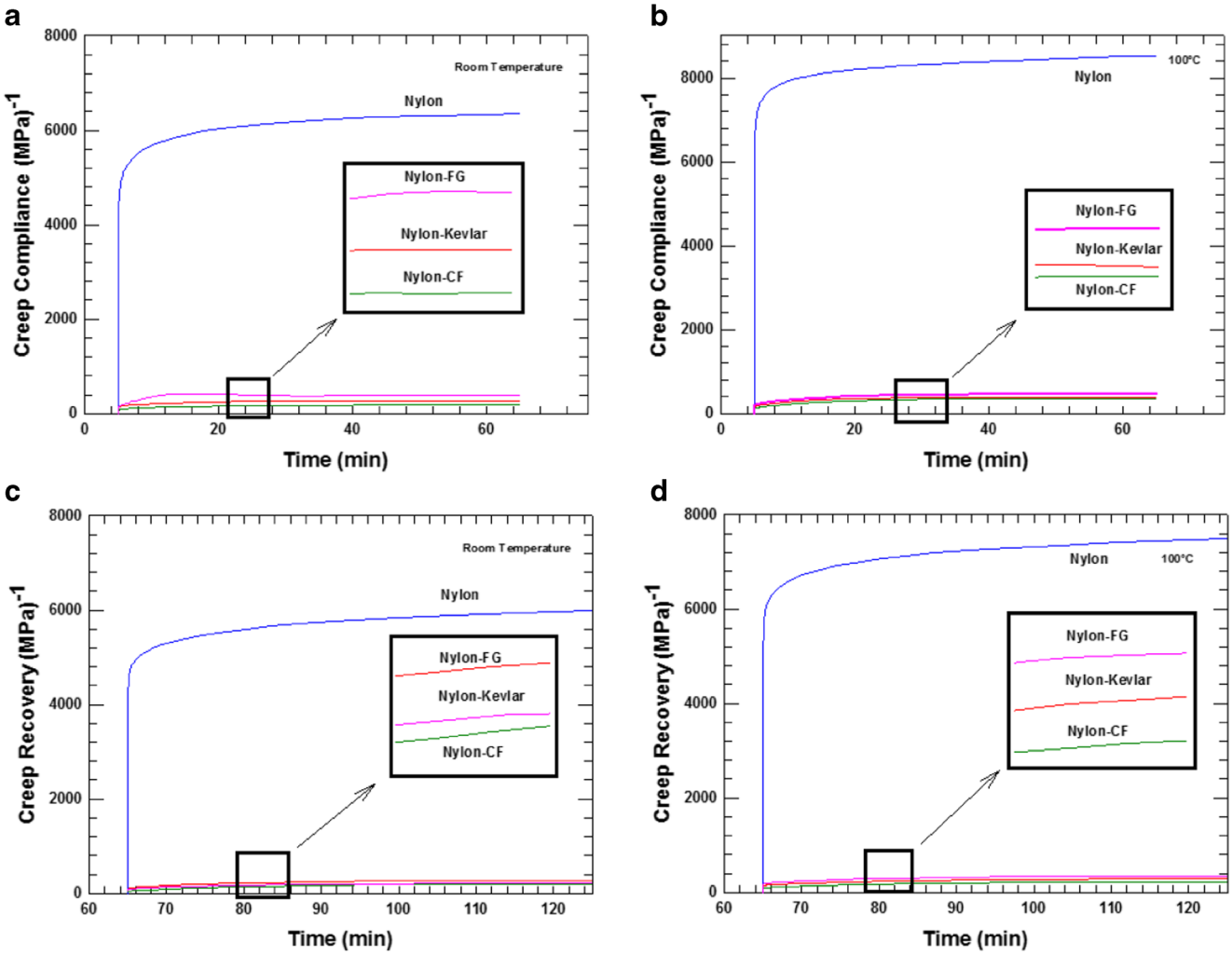

Fig. 4 **a** Creep compliance at room temperature. **b** Creep compliance at room temperature. **c** Creep recovery at 100 °C. **d** Creep recovery at 100 °C

after that nylon-Kevlar, after that nylon-FG, and finally pure nylon shows highest creep amount.

3.2 Statistical analysis

In this section, the creep results were compared statistically to confirm that there was a definite difference in the creep models for the different samples. To compare the creep models, strain and decay time of the individual samples during the static force were analyzed using regression with qualitative variables. The qualitative variable was the material type. Comparatively, Ning et al. [28] used a paired *t*-test to perform a similar but more basic analysis on the tensile strength of fiber-reinforced samples. Jiang et al. [29] studied mechanical behavior of FRAM components of three different polymers reinforced with CF. From Robinson et al. [30], creep for polymers commonly follows the Norton/Bailey power model:

$$Y = \mathrm{aX}^{b} \tag{1}$$

Note that a simple log transformation gives

$$\ln(Y) = \ln(a) + b^{*}\ln(X) \tag{2}$$

Hence, the proposed linear model is now proposed with the transformations $Y = \ln$ (strain) and X_1 = ln (decay time).

In summary, the model proposed is

$$Y = \beta\_0 + \beta\_1 X\_1 + \beta\_2 X\_2 + \beta\_3 X\_3 + \beta\_4 X\_4 + \beta\_5 X\_1 X\_2 + \beta\_6 X\_1 X\_3 + \beta\_7 X\_1 X\_4 + \epsilon \tag{3}$$

where

Y	is ln (strain)
β_0	is the intercept for nylon
X_1	is ln (decay time)
β_1	is the slope for nylon
X_2	is 0 if just nylon, 1 if CF added
β_2	is the change in the intercept from just nylon to nylon with CF

X_3 is 0 if just nylon, 1 if Kevlar added
β_3 is the change in the intercept from just nylon to nylon with Kevlar
X_4 is 0 if just nylon, 1 if FG added
β_4 is the change in the intercept from just nylon to nylon with FG
β_5 is the change in the slope from just nylon to nylon with CF
β_6 is the change in the slope from just nylon to nylon with Kevlar
β_7 is the change in the slope from just nylon to nylon with FG
ϵ is the error

From the statistical linear regression analysis, the summary in Table 1 was produced.

Results from Table 1 indicate that all samples have different creep functions based on the p values. A p value greater than 0.1 would have indicated that a variable could probably be removed from the model. Since all the p values here are showing significance, four different creep models are present. The overall R^2 of the model was 0.977, indicating that the proposed model explained 97.7% of the variability in the data. Very similar results were found for the second period of the creep analysis when the static force was removed. Again, the results indicated very strongly that the different samples had statistically different creep models. The estimates of the creep models for each specimen can be produced, from Table 1. For nylon only, the linear estimate for creep while the stress is applied is

$$\ln(Y) = 0.47731 + 0.05688^{*}\ln(X) \quad (4)$$

which transforms back into (with some rounding on the parameters for brevity)

$$Y = 1.6^{*} X^{0.06} \quad (5)$$

Table 1 Statistical linear regression analysis

Coefficients	Estimate	Standard Error	t value	p value
β 0	0.47731	0.02769	17.237	< 0.0001
β 1	0.05688	0.01178	4.828	< 0.0001
β 2	− 4.14958	0.03916	− 105.961	< 0.0001
β 3	− 3.46270	0.03916	− 88.422	< 0.0001
β 4	− 2.84812	0.03699	− 77.007	< 0.0001
β 5	0.10437	0.01666	6.264	< 0.0001
β 6	0.06407	0.01666	3.845	0.000144
β 7	0.15909	0.01497	10.629	< 0.0001

For nylon with FG added, the linear estimate for the creep while the stress is applied is

$$\ln(Y) = (0.47731 - 2.84812) + (0.05688 + 0.15909)^{*}\ln(X) \quad (6)$$

This transforms into (with some rounding on the parameters for brevity)

$$Y = 0.09^{*} X^{0.22} \quad (7)$$

For nylon with Kevlar added, the linear estimate for the creep while the stress is applied, is

$$\ln(Y) = (0.47731 - 3.46270) + (0.05688 + 0.06407)^{*}\ln(X) \quad (8)$$

This transforms into

$$Y = 0.05X^{0.12} \quad (9)$$

Finally, for nylon with CF added, the linear estimate for the creep while the stress is applied is

$$\ln(Y) = (0.47731 - 4.14958) + (0.05688 + 0.10437)^{*}\ln(X) \quad (10)$$

This transforms into the Norton/Bailey power model:

$$Y = 0.03X^{0.16} \quad (11)$$

Again, the creep models for the specimens when the stress is removed can be similarly created. For a better summary, the following graphs in Fig. 5 are presented with the given models surrounded by 95% confidence bands. In each graph, the first specimen named is represented by the top set of data. Each Norton/Bailey power model is represented by a green line, and the red lines are the 95% confidence bands. The curves are on

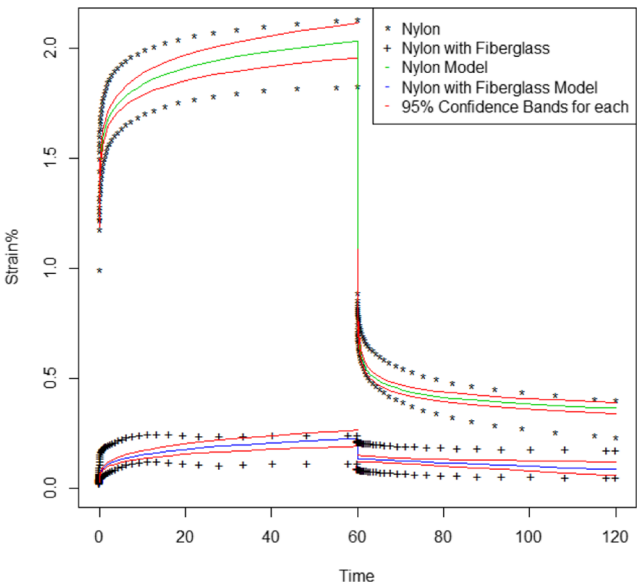

Fig. 5 Non-linear regression models for nylon versus nylon-FG

separate graphs because of the difference of scaling on the vertical strain axis. Nylon without fiber reinforcement model and experimental data (upper curves) and nylon-FG-reinforced models (lower curves) are shown in Fig. 5. It should be noted that the scale of deformation goes up to more than 2.0%. Next, nylon-Kevlar model (upper curves) and nylon-CF model (lower curves) are shown in Fig. 6. It should be noted that the strain deformation goes almost at 0.10%. Finally, nylon-FG model (upper curves) and nylon-Kevlar model (lower curves) is presented in Fig. 7. The amount of strain percentage goes to 0.25%. At high temperature, in the nylon-FG experimental data, there is a different behavior than expected, which could be because of FG being a non-organic fiber material compared with CF and Kevlar.

To summarize, there is statistical evidence that the creep models for FRAM specimens with and without reinforcing fibers of FG, Kevlar, and CF are significantly different when using the Norton/Bailey power model. Other creep models were attempted but found to be less conclusive than the Norton/Bailey model for this data. As for validity, residual diagnostics were run for all models. Again, the Norton/Bailey model was the best fitting model for this data with an R^2 of 97.7% with residuals conforming best to linear model assumptions.

3.3 Microstructural analysis

The cross section of the composite samples was observed using a microscope to study the microstructural morphology, printing quality, and fracture mechanisms. Samples were printed in a layer by layer structure of fiber and polymer, with a similar direction and printing conditions. The specimens were notched and broken using a Charpy machine according

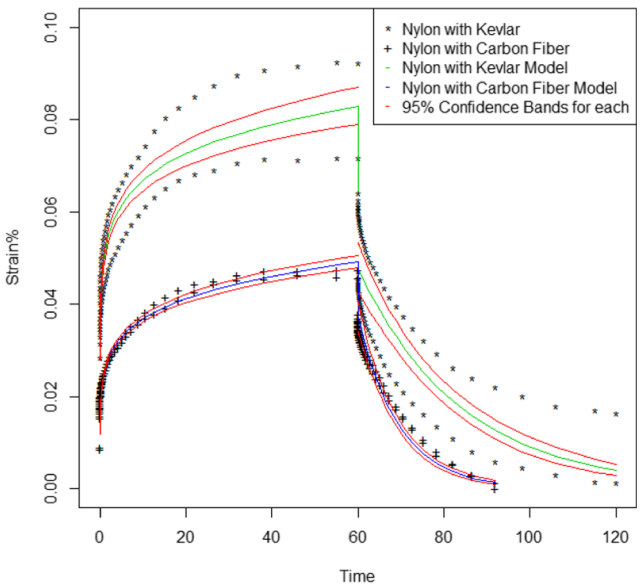

Fig. 6 Non-linear regression models for nylon, nylon-Kevlar versus nylon-CF

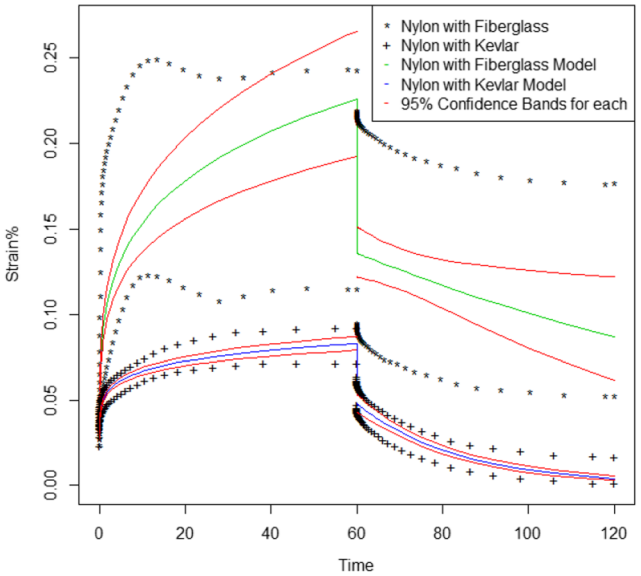

Fig. 7 Non-linear regression models for nylon-FG versus nylon-Kevlar

to the ASTM D6110-17 standard. To ensure brittle breaking, each notched sample was placed in liquid nitrogen before Charpy impact test was performed. The cross-sectional view of the broken specimens with the fiber and polymer layers is shown in Fig. 8a–d.

The interlayer adhesion between layers plays a pivotal role in determining the mechanical properties of the specimen. By increasing the interlayer adhesion, thermomechanical properties including toughness, creep, and strength can be improved [28]. Additionally, voids cause a lower binding force between layers, serve as sites for crack nucleation, and weaken the material. Furthermore, the voids created in the structure during printing processes reduce the material density and cause lower thermal, mechanical, and conductive properties [15]. In Fig. 8a, various black points are seen which appear to be voids in the pure nylon structure. In Fig. 8b–d, the bright lines represent nylon layers, while the black lines are indicative of CF, FG, and Kevlar layers, respectively.

A number of precise SEM studies has been performed to investigate the effect of the voids on creep properties. It was observed that the pure nylon specimen has a high number of voids, while the other fiber-reinforced nylon samples have almost negligible amount of voids. As can be seen from Figs. 3 and 4, the pure nylon specimen has a creep recovery and creep compliance which is almost 25 and 40 times bigger than reinforced samples. And, this finding confirms the voids provide an avenue for cracks and defects at the FRAM built products.

3.4 Discussion

FRAM creep specimens reinforced with CF, FG, and Kevlar were tested with the dynamic mechanical analysis system at different temperatures. It was observed that creep deformation

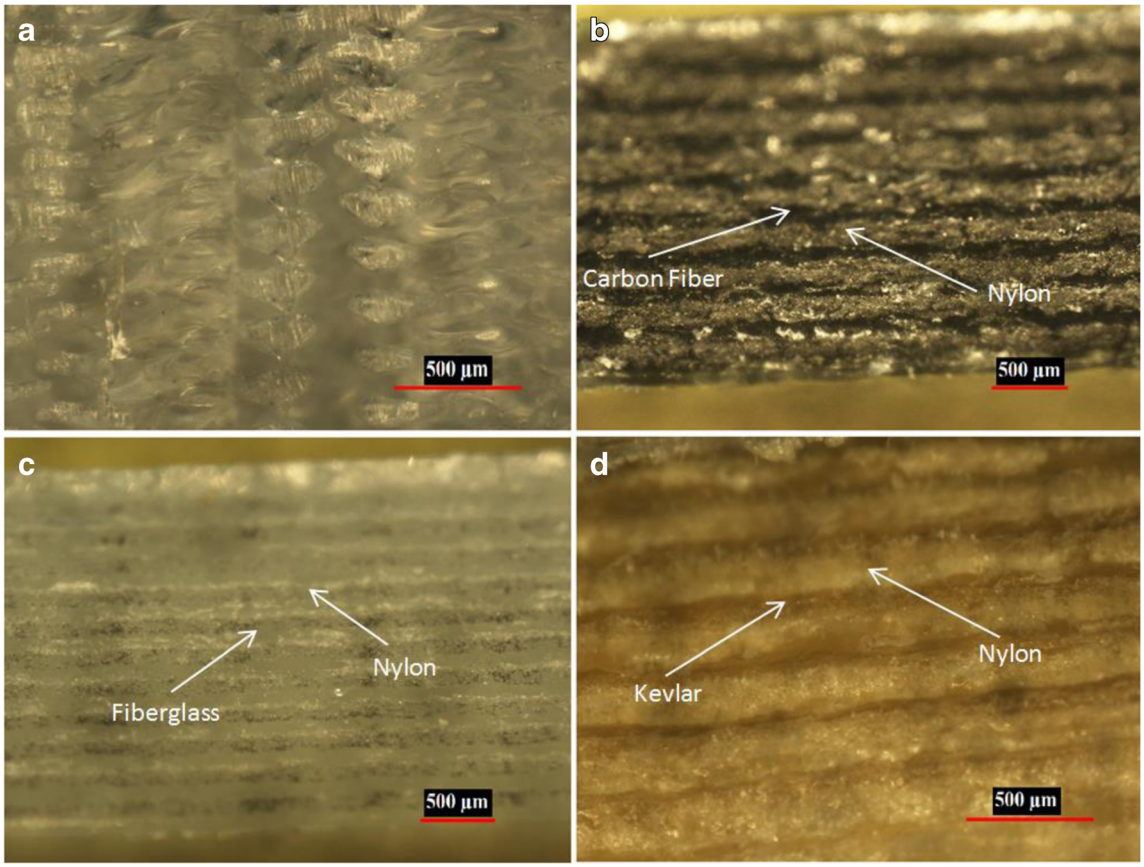

Fig. 8 Microscopic image from cross section of 3D-printed fiber-reinforced composites. **a** Pure nylon. **b** CF-nylon. **c** FG-nylon. **d** Kevlar-nylon

is temperature dependent. Viscoelastic properties of polymer determine the thermomechanical behavior of polymer composites under an applied load at different temperatures. As can be seen in Figs. 3 and 4, for all samples, as temperature increases, creep also increases because stress transfer at the interface will decrease. As test temperature increases from room temperature to 100 °C, higher than nylon Tg (about 47°C), larger free volume will become available in the structure and cause loss of interlocking between the matrix and the fiber. At temperatures below Tg, chain segments cannot move, and very little creep takes place even after a long time. At temperatures above Tg, creep strain and the rate of creep increases because of the higher macromolecular mobility in polymer chains. Polymer molecules are long-chain molecules that are tangled to each other. When creep occurs, polymer chains start to untangle and slip which cause part deformation. Many researchers presume that the polymer matrix is the ruling factor in determining the mechanical properties of composites [31–33]. The strength of the fiber-matrix interface is an important factor controlling the creep behavior. Higher temperatures weaken the bonding strength of interface and increase creep deformation [31–34]. In FRAM, due to layer by layer deposition, the structure does not provide as many tangles as normal polymers processed by injection molding have. Theoretically, mechanical properties are not as good as conventional processing methods, but inclusion of fibers improves mechanical properties to nearly the quality of conventional polymer processes [22].

The resulting creep strain is a combination of the instantaneous initial strain coming from linear elastic deformation as response to the applied stress and the non-linear viscoelastic permanent deformation increasing with the loading time. The creep compliance is greatly affected by the presence of fibers. Thus, an increase of fiber length contributes to improving the creep resistance due to a higher load transfer from the matrix to the fibers [35]. The decrease in creep compliance is observed as long as the average fiber length is higher than the critical fiber length. Because the stresses are concentrated at the fiber extremities and participate to the fiber pull out, the reduction in fiber length increases the number of fiber ends causing the composite failure. According to Schultz et al., at low temperatures or high strain rates, fiber pullout and matrix brittle fracture are the dominant failure mechanisms, while at elevated temperatures or low strain rates, failure occurred via matrix crazing and crack propagation near the fiber ends [36]. Takahashi et al. showed fiber pullouts in the longitudinal direction, while in the transverse direction, peeling of fibers is dominant. The number of fiber pullouts increases with increasing temperature [37]. In line with these studies, the fibers in the specimens used in this research study are continuous

and are longer then the critical fiber length. Thus, no fiber ends will be available causing the composite failure. Also, the load is in the axial direction, hence peeling of fibers is not dominant. The fiber concentration and orientation in the loading direction also participate to the improvement of creep resistance [35]. Further research will investigate the effect of different load and fiber directions on thermomechanical properties.

Although 3D printing is a flexible, quick, and low-cost production method, the properties of 3D-printed polymers are usually insufficient for robust engineering applications. The inclusion of reinforcing fibers is a solution which improves the thermomechanical properties greatly. Creep results of FRAM specimens support that printed parts are great candidates to replace conventional polymer composites [34, 38] and metals, especially aluminum 6061 [39, 40], for engineering applications, like automobile parts.

4 Conclusion

The main goal of this research is to increase the knowledge base of fiber-reinforced polymer composites and to further improve the strength of 3D-printed FRAM components. Nylon composites reinforced with three different fibers were produced with a MKF 3D printer. Adding CF, FG, and Kevlar fibers reduced creep in the fiber direction. The highest amount of the creep deformation was observed in the nylon sample. For other samples, creep results showed nylon > nylon-FG > nylon-Kevlar > nylon-CF. The same trend was observed for the creep recovery. In all cases, the higher the temperature, the greater the creep value for the same sample at room temperature. The statistical analysis is in concordance with the experimental values. The statistical regression analysis, with an almost 98% coefficient of determination, verified there was a difference in the creep models for the different fibers.

Acknowledgment The technical support provided by Dr. Holly Stretz, Mr. Moamen Elkelany and Mr. Garrett Perry is greatly appreciated.

Funding This study has been funded by the Center for Manufacturing Research and T.S. McCord Endowment of the College of Engineering.

References

1. Dizon JRC, Espera AH, Chen Q, Advincula RC (2018) Mechanical characterization of 3D- printed polymers. 20:44–67
2. Eftekhari M, Fatemi A (2015) Tensile, creep and fatigue behaviours of short fibre reinforced polymer composites at elevated temperatures: a literature survey. 38(12):1395–1418
3. Wang J, Li H, Liu R, Li L, Lin Y-H, Nan C-W (2018) Thermoelectric and mechanical properties of PLA/$Bi_{0.5}Sb_{1.5}Te_3$ composite wires used for 3D printing. 157
4. Ilardo R, Williams CB (2010) Design and manufacture of a Formula SAE intake system using fused deposition modeling and fiber-reinforced composite materials. 16(3):174–179
5. Chohan JS, Singh R (2016) Enhancing dimensional accuracy of FDM based biomedical implant replicas by statistically controlled vapor smoothing process. 1(1–2):105–113
6. Madhav CV, Kesav RSNH, Narayan YS (2016) Importance and utilization of 3D printing in various applications. 3(5):24–29
7. Aw Y, Yeoh C, Idris M, Amali H, Aqzna S, Teh P (2017) A study of tensile and thermal properties of 3D printed conductive ABS–ZnO composite, AIP Publishing. 1835(1):020008
8. Wang X, Jiang M, Zhou Z, Gou J, Hui D (2017) 3D printing of polymer matrix composites: a review and prospective. 110:442–458
9. Niaza KV, Senatov FS, Stepashkin AS, Anisimova NY, Kiselevsky MV (2017) Long-term creep and impact strength of biocompatible 3D-printed PLA-based scaffolds. Trans Tech Publ 13:15–20
10. Kao Y-T, Dressen T, Kim DSD, Ahmadizadyekta S, Tai BL (2015) Experimental investigation of mechanical properties of 3D-printing built composite material. 145(6):904–913
11. Gardiner G (2018) 3D printing composites with continuous fiber
12. Hopkins PM, Norris T, Chen A (2017) Creep behavior of insulated concrete sandwich panels with fiber-reinforced polymer shear connectors. 172:137–146
13. Sridhar R (2017) A review on cyclic strength of fiber reinforced soil. 12(1):33–46
14. Türk D-A, Brenni F, Zogg M, Meboldt M (2017) Mechanical characterization of 3D printed polymers for fiber reinforced polymers processing. 118:256–265
15. Quill TJ, Smith MK, Zhou T, Baioumy MGS, Berenguer JP, Cola BA, Kalaitzidou K, Bougher TL (2017) Thermal and mechanical properties of 3D printed boron nitride–ABS composites. 1–13
16. Masood S, Song W (2005) Thermal characteristics of a new metal/polymer material for FDM rapid prototyping process. 25(4):309–315
17. Hwang S, Reyes EI, Moon K-S, Rumpf RC, Kim NS (2015) Thermo-mechanical characterization of metal/polymer composite filaments and printing parameter study for fused deposition modeling in the 3D printing process. 44(3):771–777
18. Trhlíková L, Zmeskal O, Psencik P, Florian P (2016) Study of the thermal properties of filaments for 3D printing, AIP Publishing. 1752(1):040027
19. Singh R, Sandhu GS, Penna R, Farina I (2017) Investigations for thermal and electrical conductivity of ABS-graphene-blended prototypes. 10(8):881
20. De Monte M, Moosbrugger E, Quaresimin M (2010) Influence of temperature and thickness on the off-axis behaviour of short glass fibre reinforced polyamide 6.6–cyclic loading. 41:10:1368–1379
21. Mohamed OA, Masood SH, Bhowmik JL (2017) Experimental investigation of creep deformation of part processed by fused deposition modeling using definitive screening design. 18:164–17
22. Zhang H, Cai L, Golub M, Zhang Y, Yang X, Schlarman K, Zhang J (2018) Tensile, creep, and fatigue behaviors of 3D-printed acrylonitrile butadiene styrene. 27(1):57–62
23. Imeri A (2017) Investigation of the mechanical properties for fiber reinforced additively manufactured components. Tennessee Technological University, vol. MSc
24. Garg A, Bhattacharya A (2017) An insight to the failure of FDM parts under tensile loading: finite element analysis and experimental study. 120:225–236
25. Love LJ, Kunc V, Rios O, Duty CE, Elliott AM, Post BK, Smith RJ, Blue CA (2014) The importance of carbon fiber to polymer additive manufacturing. 29(17):1893–1898

26. Guessasma S, Belhabib S, Nouri H, Hassana OB (2016) Anisotropic damage inferred to 3D printed polymers using fused deposition modelling and subject to severe compression. 85:324–340
27. Forster AM (2015) Materials testing standards for additive manufacturing of polymer materials
28. Ning F, Cong W, Hu Y, Wang H (2017) Additive manufacturing of carbon fiber-reinforced plastic composites using fused deposition modeling: effects of process parameters on tensile properties. 51(4): 451–462
29. Jiang D, Smith D (2017) Mechanical behavior of carbon fiber composites produced with fused filament fabrication
30. Robinson D, Binienda W, Ruggles M (2003) Creep of polymer matrix composites. I: Norton/Bailey creep law for transverse isotropy. 129(3):310–317
31. Kogo Y, Hatta H, Kawada H, Machida T (1998) Effect of stress concentration on tensile fracture behavior of carbon-carbon composites. 32(13):1273–1294
32. Goto K, Hatta H, Takahashi H, Kawada H (2001) Effect of shear damage on the fracture behavior of carbon–carbon composites. 84(6):1327–1333
33. Hatta H, Suzuki K, Shigei T, Somiya S, Sawada Y (2001) Strength improvement by densification of C/C composites. 39(1):83–90
34. Goto K, Ohkita H, Hatta H, Iseki H, Kogo Y (2007) Tensile strength and creep behavior of carbon-carbon composites at elevated temperatures
35. Coulon A, Lafranche E, Douchain C, Krawczak P, Ciolczyk J, Gamache E (2017) Flexural creep behaviour of long glass fibre reinforced polyamide 6.6 under thermal-oxidative environment. 51(17):2477–2490
36. Schultz J, Friedrich K (1984) Effect of temperature and strain rate on the strength of a PET/glass fibre composite. 19(7):2246–2258
37. Takahashi R, Shohji I, Seki Y, Maruyama S (2014) Effect of fiber direction and temperature on mechanical properties of short fiber-reinforced PPS. IEEE:778–781
38. Sakai T, Hirai Y, Somiya S (2011) Effect of crystallinity and fiber volume fraction on creep behavior of glass fiber reinforced polyamide. Springer. pp. 159–164
39. Kahl S, Ekström H-E, Mendoza J (2014) Tensile, fatigue, and creep properties of aluminum heat exchanger tube alloys for temperatures from 293 K to 573 K (20 C to 300 C). 45(2):663–681
40. Torić N, Brnić J, Boko I, Brčić M, Burgess IW, Uzelac I (2017) Experimental analysis of the behaviour of aluminium alloy EN 6082AW T6 at high temperature. 7(4):126